06,07

Effect of an Electric Field on Phase Transitions in PZT Solid Solutions

© S.B. Vakhrushev[1,2], Yu.A. Bronwald[1]

[1] Ioffe Institute,
St. Petersburg, Russia
[2] Pacific National University,
Khabarovsk, Russia

E-mail: s.vakhrushev@mail.ioffe.ru

Received July 24, 2025
Revised July 25, 2025
Accepted August 1, 2025

The influence of an electric field on phase transitions in PZT solid-solution single crystals with low lead titanate concentration has been studied. It is shown that during cooling under an electric field exceeding a threshold value, the transition from the intermediate phase to the antiferroelectric (AFE) phase occurs via three consecutive stages. The possibility of forming an oriented AFE domain structure has been confirmed.

Keywords: antiferroelectrics, phase transitions, antiphase domains, lead zirconate titanate (PZT), X-ray diffraction.

DOI: 10.61011/PSS.2025.10.62638.212-25

1. Introduction

Today, the researchers are increasingly focused on the antiferroelectric materials. Among them, lead zirconate and its solid solutions with lead titanate (PZT, $PbZr_{(1-x)}Ti_xO_3$) are the most well-studied compounds, especially compositions with a low content of lead titanate, where a complex a sequence of phase transitions is observed including antiferroelectric (AFE) phase and intermediate ferroelectric phase with a modulated structure [1–3]. These compounds are promising for the development of high-speed capacitor energy storage devices, non-volatile memory, and electrocaloric cooling systems [4–7].

Upon cooling from the paraelectric phase, pure lead zirconate undergoes a transition to AFE phase, characterized by antiparallel displacements of lead ions and rotations of oxygen octahedra. The introduction of even a small amount of titanium stabilizes the intermediate rhombohedral phase featuring the ferroelectric properties [8,9]. Both phase transitions — to intermediate phase and to AFE phase — are characterized as first-order transitions [2,10]. As shown in [11], there are areas of phase coexistence near the points of phase transitions. The temperature range of coexistence of the intermediate and antiferroelectric phases expands with the growth of titanium content in the solid solution.

The antiferroelectric materials are featuring the antiphase domains, at the boundaries of which a phase shift of the wave of antipolar ion displacements occurs. In recent years, it has been possible to experimentally confirm the existence of antiphase domain boundaries (ADB) in pure lead zirconate [12] and in its solid solutions [13,14]. Such boundaries are narrow (about several nanometers) flat walls with nonzero polarization. They are considered as a potential basis for non-volatile memory with ultra-high recording density. The study [13] examined the effect of a weak (relative to AFE-phase destruction field) electrical field on the phase transitions and configuration of the anti-phase domains in the solid solution of $PbZr_{0.976}Ti_{0.024}O_3$ (PZT2.4). However, the measurements covered only 5 kV/cm field value. This study was aimed at identifying the field effect on transition from the ferroelectric (FE) phase into AFE-phase and on the domain structure of AFE-phase for a range of solid solutions PZT.

2. Samples and experimental techniques

In the course of the study, a series of diffraction experiments were performed to analyze Bragg scattering on single crystals of $PbZr_{0.989}Ti_{0.011}O_3$ (PZT1.1), $PbZr_{0.978}Ti_{0.022}O_3$ (PZT2.2), PZT2.4 and $PbZr_{0.96}Ti_{0.04}O_3$ (PZT4). Needle-shaped samples oriented along $\langle 110 \rangle$ direction were cut from single crystals of arbitrary shape, which were then subjected to sequential grinding and polishing followed by chemical etching in a diluted HCl solution. The prepared samples had a cross-section from 60×60 to $120 \times 120\,\mu$m, depending on the composition. Silver electrodes were applied to the end surfaces of the specimens by spraying. The samples were fixed in a specialized measuring cell, the design of which is described in detail in the study [15].

Diffraction studies were performed on a laboratory X-ray diffractometer „SuperNova“ (Rigaku Oxford Diffraction), equipped with a high-sensitivity high-resolution CCD-detector. The specimens were irradiated with the wavelengths $\lambda = 1.54$ Å (Cu-Kα) and $\lambda = 0.71$ Å (Mo-Kα).

The measurements were performed to provide a set of electric field values $0 \le E \le 5$ kV/cm. At each value of E, temperature scans were performed in the range of $313-533$ K in 3 K increments in paraelectric phase cooling mode. The thermostating was carried out by blowing with dry nitrogen using a modified Oxford Cryosystems Cobra Device system (https://oxcryo.com/products/cobra/).

Before each temperature cycle, the samples were kept in the cubic phase ($Pm\text{-}3m$) for several hours for stress relief.

For all compositions, the experiment provided an improved geometry to obtain sections of the 3D inverse space cut with a plane containing the field application direction $\langle 110 \rangle$. All experimental data were interpreted within the framework of cubic crystal system ($Pm\text{-}3m$).

The phase transitions were identified based on the analysis of intensity of various superstructural reflections, as well as by the nature of splitting of the main Bragg reflections, for which a dedicated program was used „pi-map“ [16].

3. Results and discussion

3.1. Types of superstructural reflections in PZT

In solid solutions of PZT with a titanate content $x \leq 0.05$, the transition to the antiferroelectric phase occurs through an intermediate quasi-rhombohedral phase (IP) [1,8,17]. A characteristic feature of IP is the presence of superstructural reflections described by the reciprocal lattice vector $\tau_{\mathrm{M}} = [h{+}1/2\ \ k{+}1/2\ \ l]$, corresponding to M-point of Brillouin zone of the cubic phase, and hereinafter referred to as the M-superstructure. The intensity of the superstructural reflections I_M is proportional to the square of the antiferrodistortive parameter of η_M^2 order and concentration of the intermediate phase C_{IP}.

When transiting from the IP phase to AFE-phase the superstructural reflections of Σ-type are generated, delineated by the reciprocal lattice vector$\tau_{\Sigma} = [h{+}1/4\ k{+}1/4\ l]$. Their intensity is determined by the product of the square of AFE-phase order parameter η_{AFE}^2 by its concentration C_{AFE}. Thus, the analysis of the temperature dependence of the intensity of superstructural reflections of both types is a reliable method for monitoring transitions between the intermediate and AFE phases.

3.2. Phase transformations in electric field: transition from the intermediate to the antiferroelectric phase in the cooling mode

When cooled in the absence of electric field (ZFC mode), all the studied samples showed structural transitions, the temperatures of which are in good agreement with the experimental data [1,17,18]. In case of PZT1.1 crystal the intermediate phase was observed that existed in a narrow temperature range (< 20 K). When cooling, even in the 5 kV/cm field, only a slight shift in the transition to low temperatures was observed. In case of PZT4, a wide temperature window of coexistence of M-type and Σ-type reflexes was observed, which made it difficult to accurately determine the temperatures of phase transitions.

Of particular interest are the results obtained for compositions PZT2.2 and PZT2.4. Figure 1 illustrates the temperature dependencies of the superstructural reflection intensity (0.5 0 −1.5) for PZT2.2 single crystal when

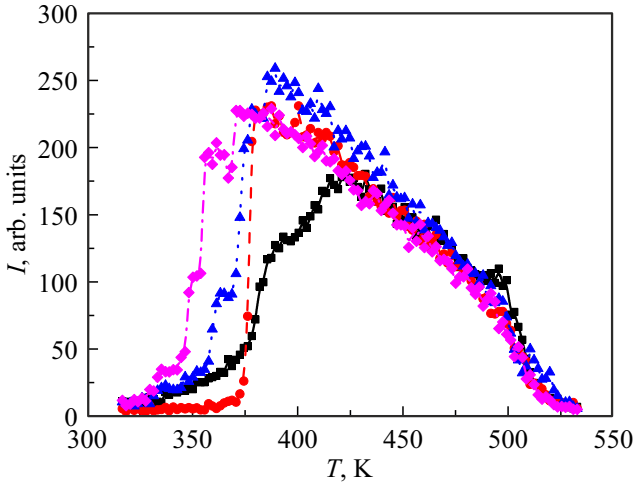

Figure 1. Temperature evolution of the intensity of a superstructural reflection $[0.5\ 0\ \overline{1.5}]$ for the single crystal PZT2.2 measured during cooling without external field (black squares, solid line) and with application of electrical field of 1 kV/cm (red dots, dashed line), 3 kV/cm (blue triangles, dashed line) and 5 kV/cm (violet rhombs, dashed line.

cooled in zero field and in the fields with intensity from 1 kV/cm to 5 kV/cm (the results for PZT2.4 are equivalent). In zero field, there is a wide transition region from the ferroelectric to antiferroelectric phase, and the analysis of reflections of M- and Σ-types clearly indicates the existence of a two-phase region. Abnormally wide Σreflections indicate a submicron size of the AFE phase regions. Because of this smearing it becomes difficult to precisely determine the temperature of transition to AFE phase. The broadening of the transition from FE phase to AFE phase in the cooling mode was previously demonstrated in papers [11,17]. In paper [11] the transition was described as a smeared one, and it was shown that the interval of coexistence of phases in $PbZr_{0.98}Ti_{0.02}O_3$ was more than 50 K. The application of even a weak field (1 kV/cm) leads to a sharp change in the nature of the transition, shifting it towards low temperatures and making the transition more abrupt (Figure1).

A detailed study of the effect of the electric field ($E > 1$ kV/cm) revealed a complex pattern of phase transformations. Two or three steps appear on the temperature dependences of the intensity of superstructural reflections, corresponding to the splitting of the phase transition into three consecutive transitions at temperatures $T1 > T2 > T3$. This phenomenon is explained by the presence of domains in the crystal with different orientation of the polarization vectors relative to the field direction. In this case, the step corresponding to $T1$ (associated with domains having a negative polarization projection on the field direction) is absent in some cases, which may be due to the disappearance of such domains upon cooling from paraphase. In particular, in [13], only two transitions were observed when PZT2.4 crystal was cooled in the field

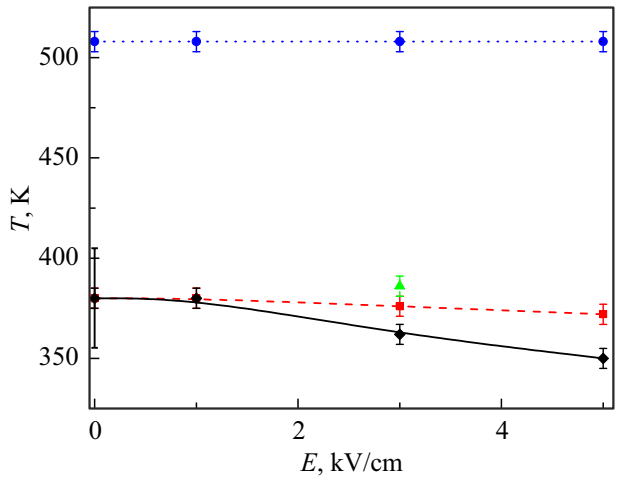

Figure 2. Temperature of phase transitions of PZT2.2 single crystal versus magnitude of the applied electric field in the cooling process. Blue squares and dashed line — temperature of transition from paraelectric phase to FE phase; red dots and dashed line — $T2$ $(\mathbf{P}\cdot\mathbf{E}=0)$; black squares and solid line — $T3$ $(\mathbf{P}\cdot\mathbf{E}>0)$; green triangle — $T1$ $(\mathbf{P}\cdot\mathbf{E}<0)$. In zero field $(E=0)$ the solid vertical line denotes the smeared transition from PE-phase to AFE-phase.

of 5 kV/cm. In Figure 1 all three transitions are identified only for the field 3 kV/cm. Figure 2 shows the transition temperatures versus the applied field. The temperature $T2$ is weakly dependent on the magnitude of the applied field, whereas $T3$ declines with the growth of the field strength, which is in good agreement with the study [13]. The smeared region of transition from FE-phase to AFE-phase at zero field is highlighted by a vertical stripe.

Let us consider in more detail the mechanism of the electric field effect on the transition temperature. The transition temperature between the FE and AFE phases is determined by the intersection point of the temperature dependences of the free energies of these phases [19]. Assuming that the electric field has little effect on the energy of AFE phase, it can be suggested that the change in the transition temperature ΔT is completely determined by the change in FE phase energy under the action of electric field ΔF. For the small fields we may assume $\Delta T \propto \Delta F$.

Let's write down the expression for the free energy of a ferroelectric in electric field [20,21]:

$$F(T,E) = F_0(T) + \mathbf{P}(T,E)\cdot\mathbf{E}$$

Here $F_0(T)$ — free energy in the absence of electric field, $\mathbf{E}$ — external electric field, T — temperature. The temperature- and field-dependent polarization $\mathbf{P}(T,E) = \mathbf{P}_{sp}(T) + \mathbf{P}_{ind}(T,E)$ includes the temperature-dependent spontaneous part $\mathbf{P}_{sp}(T)$ and the temperature- and field-dependent induced polarization $\mathbf{P}_{ind}(T,E)$, which, when the fields are not too large, is usually significantly less than the spontaneous one [21]. The dependence turns out to be significantly nonlinear, which is due to the fact that $\mathbf{P}_{sp}$ increases with the decreasing temperature.

3.3. Antiphase domains and domain boundaries

The antiferroelectric order parameter can be correlated with one of twelve possible wave vectors $q_{AFE} = \{1/4\ 1/4\ 0\}$ (in $2\pi/a$ units, where a is the parameter of a pseudocubic lattice), while the domain states described by the wave vectors $\pm q_{AFE}$, are equivalent. The intensity of superstructural reflections of Σ type is proportional to the product of the square of the order parameter η_{AFE} on the occupancy of the corresponding domain states. A comparative analysis of the intensity of reflections makes it possible to quantify their occupancy.

We've analyzed the scattering patterns for PZT1.1, PZT2.2 and PZT2.4 samples. In case of PZT4 , the FE phase persisted to room temperature and the AFE domains were not studied.

As expected, cooling of the pre-annealed samples from the paraelectric phase in zero field for all compositions resulted in almost equally probable formation of six possible antiferroelctric domain states with antiferroelectricity vectors $\mathbf{A}_1 = (110)$, $\mathbf{A}_2 = (1\bar{1}0)$, $\mathbf{A}_3 = (101)$, $\mathbf{A}_4 = (10\bar{1})$, $\mathbf{A}_5 = (011)$, $\mathbf{A}_6 = (01\bar{1})$, which is in good consistency with the data from [13]. As an example, Figure 3, *a* shows a cross-section of the reciprocal space with a plane $(h\,0\,l)$ in the vicinity of the node $(\bar{2}00)$ of PZT1.1 crystal cooled in zero field at 324,K. In this geometry, the reflections are observed corresponding to the vectors $\mathbf{A}_3$ (points α and δ in the figure) and $\mathbf{A}_4$ (points β and γ in the figure). The intensity of these reflections turns out to be almost the same. For quantitative comparison, a one-dimensional scan through the points γ and δ is shown (Figure 3, *c*). It is clearly seen that the peaks have almost identical intensities. Reflections corresponding to vectors $\mathbf{A}_1$, $\mathbf{A}_2$, $\mathbf{A}_5$ and $\mathbf{A}_6$ (not shown in the figure) had approximately the same intensity. The same case was observed in PZT2.2 and PZT2.4 crystals.

Cooling in the $E \geq 3$ kV/cm field leads to a significant redistribution of the intensities of superstructural reflections, which indicates a change in the occupancy of the corresponding domain states. Figure 3, *b* illustrates a cross-section of the reciprocal space cut with plane $(h\,0\,l)$ in the vicinity of $(\bar{2}00)$ of PZT1.1 crystal cooled in the field of 5 kV/cm at a temperature of 324 K, while Figure 3, *d* showed a 1D scan passing through the points γ and δ. Reflections β and γ corresponding to the vector $\mathbf{A}_4$ directed perpendicular to the field are enhanced, while reflections α and δ are significantly weakened. The intensity of reflections $\mathbf{A}_4$ makes about 80 % of the total intensity of the superstructural reflections corresponding to the antiferroelectric phase (peaks corresponding to AFE-domains $\mathbf{A}_5$ and $\mathbf{A}_6$ were measured near the angle (002)). PZT2.2 crystal demonstrated absolutely the same results with the total occupancy of domain$\mathbf{A}_4 \sim 65$ %. The results obtained are consistent with the findings of paper [13].

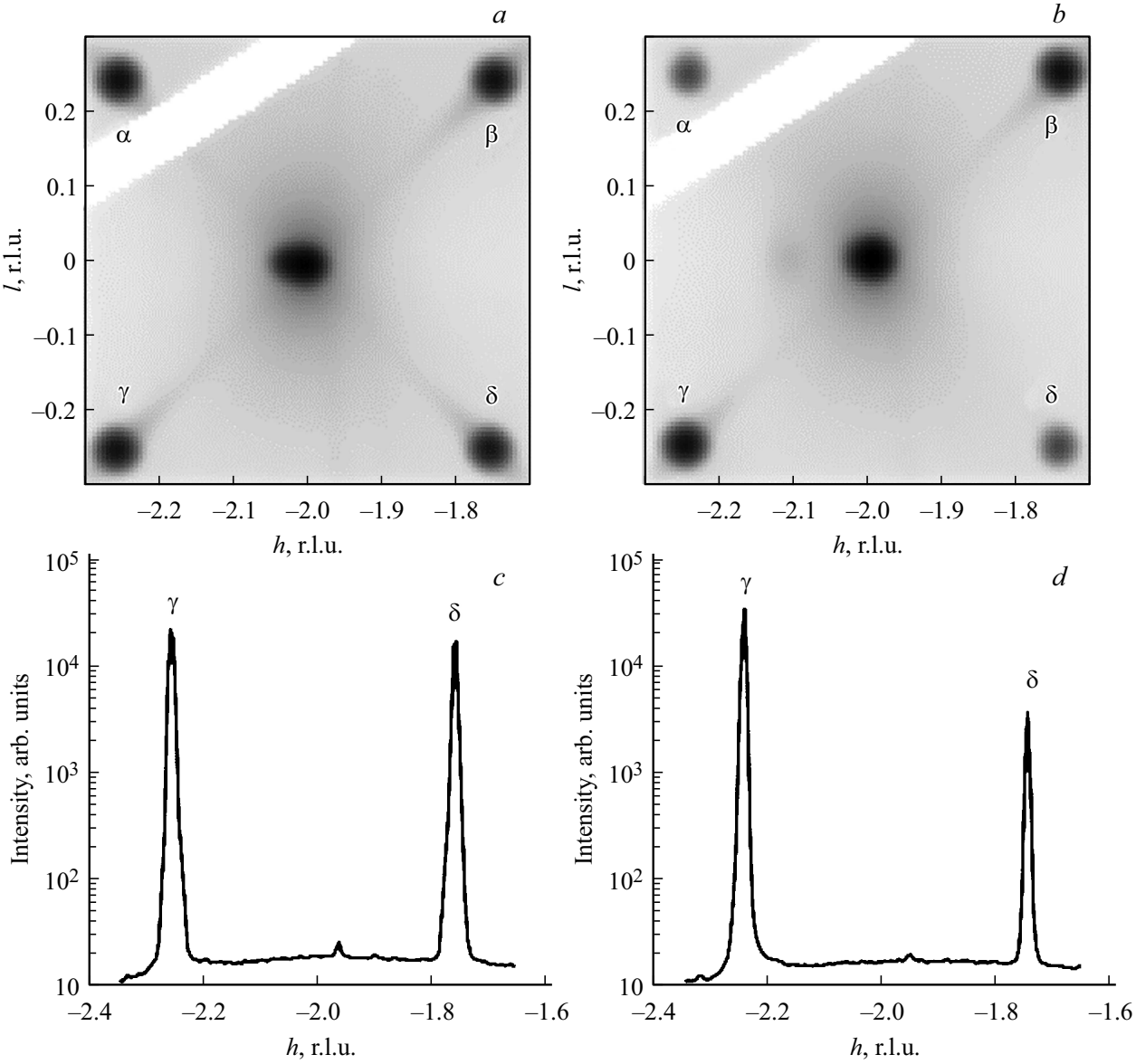

Figure 3. (*a*) — section of the reciprocal space cut by $(h\,0\,l)$ plane in the vicinity of $(\bar{2}00)$ of PZT1.1 crystal when cooled in zero field, (*b*) — in the field 5 kV/cm, (*c*) — 1D scan through the points γ and δ at $E = 0$, (*d*) — 1D scan through the points γ and δ at $E = 5$ kV/cm.

4. Conclusion

• It was confirmed that in solid solutions of PZT, the phase transition from the rhombohedral ferroelectric phase to the anti-ferroelectric phase (FE→AFE) when cooled in electric field applied in the direction {110} occurs through three distinct stages, which is associated with different orientation of the field with respect to spontaneous polarization. The dependence of the transition temperature shift on the magnitude of the field is nonlinear. This is due to the fact that lower transition temperatures lead to higher spontaneous polarization. The discovered effect should be common to any crystals undergoing a reverse transition from polar to the nonpolar phase.

• It was demonstrated that cooling of PZT crystals containing titanium $x \leq 2.4$ in the electric field with intensity of ≥ 3 kV/cm, applied along {110}, results in a clearly manifested anisotropy of the domain structure in the antiferroelectric phase. The domain state is selectively stabilized with the antiferroelectric vector **A** perpendicular to the field, while other domain states are suppressed.

• The effect of selective stabilization of the domain structure was observed in all the crystals studied, regardless of the width of the region of existence of the intermediate phase. Due to this observation, we may suggest that presence of the intermediate FE phase is not a necessary precondition for controlling the electric field of the AFE phase domain structure, and the effect should be observed

in pure lead zirconate, as well. The possibility of controlling the antiferroelectric domain structure in epitaxial films remains a pivotal issue.

Funding

This study was funded by the Ministry of Science and Higher Education of the Russian Federation (project No. FEME-2024-0005).

Conflict of interest

The authors declare that they have no conflict of interest.

References

[1] N.G. Leontiev, O.E. Fesenko, V.G. Smotrakov. FTT **25**, *7*, 1958 (1983).
[2] R.W. Whatmore, A.M. Glazer. J. Phys. C: Solid State Phys. **12**, *8*, 1505 (1979).
[3] H. Fujishita, S. Hoshino. J. Phys. Soc. Jpn **53**, *1*, 226 (1984).
[4] Ch.W. Ahn, G. Amarsanaa, S.S. Won, S.A. Chea, D.S. Lee, I.W. Kim. ACS Appl. Mater. Interfaces **7**, *48*, 26381 (2015).
[5] K.M. Rabe. Functional metal oxides: new science and novel applications. Wiley-VCH, Weinheim (2013). P. 221.
[6] Xi. Hao. J. Adv. Dielectr. **3**, *1*, 1330001 (2013).
[7] X.-K. Wei, A.K. Tagantsev, A. Kvasov. Nat. Commun. **5**, *1*, 3031 (2014).
[8] S. Watanabe, Y. Koyama. Phys. Rev. B **63**, *13*, 134103 (2001).
[9] S. Watanabe, Y. Koyama Physical Review B, **66**, *13*, 134102 (2002).
[10] H. Fujishita, S. Tanaka. Ferroelectrics **258**, *1*, 37 (2001).
[11] J. Handerek, J. Kwapuliniski, M. Pawelczyk, Z. Ujma. Ph. Transit. **6**, *1*, 35 (1985).
[12] X. Wei, A.K. Tagantsev, A. Kvasov, K. Roleder, Ch. Jia, N. Setter. Nat. Commun. **5**, *1*, 1 (2014).
[13] S.B. Vakhrushev, D. Andronikova, I. Bronwald, E.Y. Koroleva, D. Chernyshov, A.V. Filimonov, S.A. Udovenko, A.I. Rudskoy, D. Ishikawa, A.Q.R. Baron, A. Bosak. Phys. Rev. B **103**, *21*, 214108 (2021).
[14] S. Vakhrushev, D.A. Andronikova, D.Y. Chernyshov, A.V. Filimonov, S.A. Udovenko, N.R. Kumar. In: International Conference on Next Generation Wired/Wireless Networking. Springer International Publishing, Cham (2018). P. 683.
[15] S.A. Udovenko, D.Yu. Chernyshov, D.A. Andronikova, A.V. Filimonov, S.B. Vakhrushev. FTT **60**, *5*, 960 (2018). (in Russian).
[16] Software ≪Program for getting the scattering intensity distributions in coordinates omega-2theta „pi-map“ RQ, license holder: FSAEI HE „SPbPU“, № 2017617111.
[17] K. Roleder. Key Eng. Mater. **155**, *1*, 123 (1998).
[18] D. Viehland, J.F. Li, X. Dai, Z. Xu. J. Phys. Chem. Solids **57**, *10*, 1545 (1996).
[19] L. D. Landau and E. M. Lifshitz, Teoreticheskaya fizika. Statisticheskaya fizika. Butterworth-Heinemann (1976). p. 584. (in Russian).
[20] W.J. Merz. Phys. Rev. **91**, *3*, 513 (1953).
[21] G.A. Smolensky, V.A. Bokov, V.A. Isupov, N.N. Kraynik, R.E. Pasynkov, M.S. Shur. Segnetoelektriki i antisegnetoelektriki. L.: Nauka, Leningr. (1971) p. 476. (in Russian).

Translated by T.Zorina